Al-Azhar Bulletin of Science

Volume 34 | Issue 1 Article 4

2023

Section: Mathematics and Statistics

VIBRATIONS REDUCTION OF A CLAMPED- CLAMPED MICRO-BEAM VIA POSITIVE POSITION FEEDBACK CONTROLLER

H. Mosaa
Department of Mathematics, Faculty of Science(Girls Branch) , Al-Azhar University, Egypt.,
heba.elsayed@azhar.edu.eg

M. Kamel
Department of Physics and Engineering Mathematics, Faculty of Electronic Engineering, Menofia University, Egypt

H. El Gohry
Department of Physics and Engineering Mathematics, Faculty of Electronic Engineering, Menofia University, Egypt

L. S. Diab
Department of Mathematics, Faculty of Science(Girls Branch) , Al-Azhar University, Egypt.

H. M. Shawky
Department of Mathematics, Faculty of Science(Girls Branch) , Al-Azhar University, Egypt.

How to Cite This Article

Mosaa, H.; Kamel, M.; El Gohry, H.; Diab, L. S.; and Shawky, H. M. (2023) "VIBRATIONS REDUCTION OF A CLAMPED- CLAMPED MICRO-BEAM VIA POSITIVE POSITION FEEDBACK CONTROLLER," *Al-Azhar Bulletin of Science*: Vol. 34: Iss. 1, Article 4.
DOI: http://doi.10.21608/absb.2022.169571.1210

VIBRATIONS REDUCTION OF A CLAMPED- CLAMPED MICRO-BEAM VIA POSITIVE POSITION FEEDBACK CONTROLLER

Cover Page Footnote

Acknowledgments The author would like to thank the department of mathematics, faculty of Science(Boys), Al-Azhar university, for supporting this study.

ORIGINAL ARTICLE

Vibration Reduction of a Clamped−Clamped Microbeam Through a Positive Position Feedback Controller

Heba Mosaa [a,*], Magdy Kamel [b], Hany El-Gohry [b], Lamiaa Sabry Diab [a], Hamida Mohamed Shawky [a]

[a] Department of Mathematics, Faculty of Science (Girls Branch), Al-Azhar University, Egypt
[b] Department of Physics and Engineering Mathematics, Faculty of Electronic Engineering, Menofia University, Egypt

Abstract

This manuscript displays the vibration reduction of a clamped−clamped microbeam subjected to an excitation external force through applying the positive position feedback (PPF) controller. The approximate solutions of the whole system are obtained up to the second-order approximation with the help of the multiple-scale perturbation technique (MSP). The stability analysis is studied by utilizing the frequency response equations near the simultaneous condition $(\Omega = \omega_1, \omega_1 = \omega_2)$. Time histories and response curve figures before and after control of the whole system are examined numerically using the Runge-Kutta Fourth-order method (Maple(16) software and Matlab 7.7(R2014) software. Numerical results of the influences of different parameters and the whole system behavior are investigated at the worst resonance case to display the optimum conditions of decreasing the vibrations. The acquired results revealed that the PPF controller plays a significant role in reducing the studied system oscillations. The effectiveness of the controller E_a was about 162, means that the controller reduced the vibration to about 99.40%. A comparison between the numerical and approximate solutions is presented to appear the validity of the results.

Keywords: Frequency response, Microbeam, Perturbation technique, PPF controller, Resonance, Stability

1. Introduction

Vibrations displayed in many applications such as beam structures, structural systems, and turbomachinery are considered an undesired phenomenon as they may cause noise, failure, damage, and on occasion demolish the whole systems. Nevertheless, they are occasionally coveted. So, in order to repress the oscillations of various nonlinear structures, numerous controllers are utilized, including time delay control, and passive and active control techniques. Ekici and Boyaci [1] discussed the microbeam oscillations of two different subharmonic and super-harmonic resonances by using the perturbation approach. Through that discussion, they clearly show that the limit conditions have an effect on framework oscillations. Moreover, several researcher efforts are loaded out for discussing the microbeam behavior in micro-electrical mechanical system (MEMS) appliances [2−4]. Also, in Ref. [5], the microbeam response when sandwiched between two electrodes is examined. To get the motion's equation, they used the Galerkin technique. The perturbation technique was utilized for solving the nonlinear differential motion equation. All resonance cases are discussed. For studying the effect of the different parameters on the response curves of the entire system, they used the parametric sensibility study.

Recent years have seen a rise in interest in the discussion of different oscillating nonlinear systems [6−10]. In numerous articles, the time delay was used to minimize nonlinear structure oscillations. Liu et al. [11] studied the effect of a mix of

Received 25 October 2022; revised 13 December 2022; accepted 14 December 2022.
Available online 18 August 2023

* Corresponding author at: Department of Mathematics, Faculty of Science (Girls Branch), Al-Azhar University, Egypt.
E-mail address: heba.elsayed@azhar.edu.eg (H. Mosaa).

https://doi.org/10.58675/2636-3305.1641

displacement delay and velocity delay controllers on a cantilever beam. They have the ability for determining all of super-harmonic and subharmonic resonance cases with the help of the multiple scales approach. Also, the authors in Ref [12] displayed a study of the effect of displacement delay and velocity delay with a PD controller in a rotating beam. They were able to deduce that the time delay with a PD controller is superior to the active control without delay in repression oscillations in this system. Moreover, Hamed et al. [13,14] used both time delay with PPF or PD controllers subjected to a multi-excitation atomic force microscopy (AFM) paradigm for extracting the delay effects on the oscillation control's operation.

As the goal of most studies strives to repress vibrations, one of the most successful approaches in active vibration control's domain is the PPF controller. A lot of researchers have dedicated all of their time to enhance the PPF controller's performance. Amer et al. [15,16] presented a study of the influence of PPF controller under harmonic excitation on a nonlinear beam and a nonlinear system in the existence of simultaneous resonance. They deduced that the controller can minimize the oscillations in Ref. [15] by about 99.98% and in Ref. [16] by about 99.93% from their values before control. A modified PPF control was offered as an alternative to the traditional PPF by Mahmoodi and Ahmadian [17]. For damping and repression, they utilized first-order and second-order oscillators, respectively. Omidi et al. [18] showed that the effect of multi-positive feedback (MPF) approach on flexible constructions. They compared the outcomes obtained by the novel nonlinear MPPF with those obtained by the traditional PPF. Nonlinear oscillations for flexible constructions and cantilever beam can be minimized [19,20], utilizing the nonlinear modified positive position feedback (NMPPF). Their results deduced that the nonlinear MPPF has a notable role in suppression performance, and it is more effective in minimizing the oscillations than the PPF. Also, Mohanty and Dwivedy [21] discussed the vibration suppression of a nonlinear spring-mass primary system under external and parametric excitations through applying the modified traditional and nontraditional nonlinear absorber. Utilizing the multiple scales method, they derived the equations of motion at simultaneous parametric, primary, super harmonic with 1:1 internal resonance case. They achieved by their results to reduce vibrations by about 100% from its value before adding the control for a certain range of operating frequencies. Zhang and Chen [22] presented a study of applying two modified nonlinear saturation-based controllers (MNSC) and negative velocity feedback controller (NVF) to repress vibrations of a horizontally supported Jeffcott-rotor system. They utilized the integral equation method to obtain the analytical solutions up to the second-order approximations. They reached to reduce vibrations to 99.8% by using the proposed MNSC and NVF control that can repress the transient vibrations and prohibit the main system to have big amplitude vibration. Moreover, Saeed et al. [23] applied a novel control technique of the propotional-derivative (PD) controller along with the eight-poles electromagnetic actuator for suppressing vibrations of the nonlinear Jeffcott-rotor system. They derived the analytical results by utilizing the perturbation technique up to the first-order approximation. They illustrated that the Jeffcott-rotor system before utilizing the control can display stable symmetrical motion besides great vibration amplitudes for horizontal and vertical directions. Also, they acquired that the improper design of the gains of the controller can destabilize the Jeffcott system and force it to perform either chaotic or quasiperiodic motions.

The article's study plan is as follows: In Section 2, the microbeam system's mathematical modeling after adding the PPF control is discussed, thereafter employing the (MSP) approach to obtain approximate solutions up to the second-order approximation. In Section 3, stability investigation is studied by utilizing the equations of frequency response. In Section 4, the results and discussions are presented. The effect of different parameters on the oscillating microbeam system before and after the control are examined. In addition, we observed all foretelling from the analytical solutions and numerical ones agree fairly well. Lastly, Section 5 displays the conclusions.

2. Mathematical modeling

The graphic paradigm of the clamped−clamped microbeam is displayed in Fig. 1. The dominating motion's equation of the oscillating microbeam system is discussed in Ref. [5]. The dynamical model of the microbeam system motion's equation may be modified by appending another equation of the PPF controller displayed by

$$\ddot{u}+\mu_1\dot{u}+{\omega_1}^2u+\alpha_1u^4\ddot{u}+\alpha_2u^2\ddot{u}+\alpha_3u^3+\alpha_4u^5+\alpha_5u^7=F\cos(\Omega t)+\mathrm{k}_1v \tag{1}$$

$$\ddot{v}+\mu_2\dot{v}+{\omega_2}^2v=k_2u \tag{2}$$

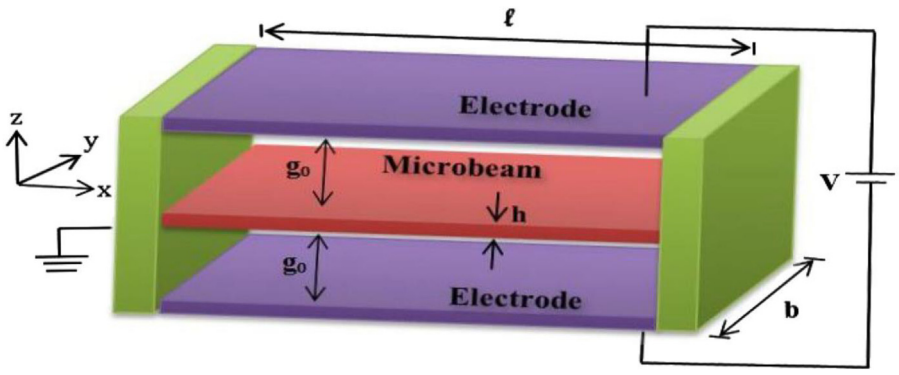

Fig. 1. Graphic paradigm for the clamped–clamped microbeam beam.

where u and v are the displacement of the microbeam system and the PPF controller, respectively; μ_1, μ_2 are the damping coefficients; $\omega_1 = \frac{a_4}{a_3}, \omega_2$ are the natural frequencies; $\alpha_1 = \frac{a_1}{a_3}, \alpha_2 = \frac{a_2}{a_3}, \alpha_3 = \frac{a_5}{a_3}, \alpha_4 = \frac{a_6}{a_3}, \alpha_5 = \frac{a_7}{a_3}$ are the nonlinear parameters; the terms $a_s (s = 1, ...7)$ are presented in Ref. [5]; F is the excitation forcing amplitude; Ω is the excitation frequency of the microbeam system,; k_1, k_2 are the control and feedback signal gains of the microbeam system and the PPF controller, respectively; and ε is a perturbation parameter.

2.1. Perturbation analysis

As the parameters of the microbeam system appear in the next perturbation equations, the previous parameters are scaling as follows:

$$\mu_1 = \varepsilon\widehat{\mu}_1, \mu_2 = \varepsilon\widehat{\mu}_2, \alpha_1 = \varepsilon\widehat{\alpha}_1, \alpha_2 = \varepsilon\widehat{\alpha}_2, \alpha_3 = \varepsilon\widehat{\alpha}_3, \alpha_4 = \varepsilon\widehat{\alpha}_4, \alpha_5 = \varepsilon\widehat{\alpha}_5, F = \varepsilon\widehat{F}, k_1 = \varepsilon\widehat{k}_1, k_2 = \varepsilon\widehat{k}_2$$

Utilizing the MSP) approach [24,25].

$$\mathrm{u}(t;\varepsilon) = u_0(T_0, T_1, \mathrm{T}_2) + \varepsilon\, u_1(T_0, T_1, \mathrm{T}_2) + \varepsilon^2 \mathrm{u}_2(T_0, T_1, \mathrm{T}_2) \tag{3}$$

$$\mathrm{v}(t;\varepsilon) = v_0(T_0, T_1, \mathrm{T}_2) + \varepsilon \mathrm{v}_1(T_0, T_1, \mathrm{T}_2) + \varepsilon^2 \mathrm{v}_2(T_0, T_1, \mathrm{T}_2) \tag{4}$$

Time derivatives are given by

$$\frac{d}{dt} = D_0 + \varepsilon D_1 + \varepsilon^2 \mathrm{D}_2, \frac{d^2}{dt^2} = {D_0}^2 + 2\varepsilon D_0 D_1 + \varepsilon^2\left({D_1}^2 + 2D_0 D_2\right) \tag{5}$$

Substituting equations (3)–(5) into equations (1) and (2) and then comparing the parameters of ε as follows:

$$\varepsilon^0 : \left({D_0}^2 + {\omega_1}^2\right)\mathrm{u}_0 = 0 \tag{6a}$$

$$\left({D_0}^2 + {\omega_2}^2\right)\mathrm{v}_0 = 0 \tag{6b}$$

$$\varepsilon^1 : \left({D_0}^2 + {\omega_1}^2\right)\mathrm{u}_1 = -2D_0 D_1 u_0 - \widehat{\mu}_1 D_0 u_0 - \widehat{\alpha}_1 \left({\mathrm{u}_0}^4 \left({D_0}^2 u_0\right) - \widehat{\alpha}_2 \left({\mathrm{u}_0}^2 \left({D_0}^2 u_0\right) - \widehat{\alpha}_3\, {\mathrm{u}_0}^3\right.\right.$$

$$-\widehat{\alpha}_4\, {\mathrm{u}_0}^5 - \widehat{\alpha}_5\, {\mathrm{u}_0}^7 + \widehat{F}\cos(\Omega t) + \widehat{k}_1 v_0 \tag{7a}$$

$$\left({D_0}^2 + {\omega_2}^2\right)\mathrm{v}_1 = -2D_0 D_1 v_0 - \widehat{\mu}_2 D_0 v_0 + \widehat{k}_2 u_0 \tag{7b}$$

$$\varepsilon^2 : \left({D_0}^2 + {\omega_1}^2\right)\mathrm{u}_2 = -2D_0 D_1 u_1 - {D_1}^2 u_0 - 2D_0 D_2 u_0 - \widehat{\mu}_1 (D_0 u_1 + D_1 u_0) - \widehat{\alpha}_3 \left(3{u_0}^2 u_1\right)$$

$$-\widehat{\alpha}_1 \left[{u_0}^4 \left({D_0}^2 u_1 + 2D_0 D_1 u_0\right) + 4u_1 {u_0}^3 \left({D_0}^2 u_0\right)\right] - \widehat{\alpha}_4 \left(5u_1 {u_0}^4\right) - \widehat{\alpha}_5 \left(7{u_0}^6 u_1\right)$$

$$-\widehat{\alpha}_2 \left[{u_0}^2 \left({D_0}^2 u_1 + 2D_0 D_1 u_0\right) + 2u_1 u_0 \left({D_0}^2 u_0\right)\right] + \widehat{\mathrm{k}}_1 v_1 \tag{8a}$$

$$\left({D_0}^2 + {\omega_2}^2\right)\mathrm{v}_2 = -2D_0 D_1 v_1 - {D_1}^2 v_0 - 2D_0 D_2 v_0 - \widehat{\mu}_2 (D_0 v_1 + D_1 v_0) + \widehat{\mathrm{k}}_2 u_1 \tag{8b}$$

The general solutions of equation (6), are presented through:

$$u_0 = A(T_1, \mathrm{T}_2)\mathrm{e}^{i\omega_1 T_0} + \overline{A}(T_1, \mathrm{T}_2)\mathrm{e}^{-i\omega_1 T_0} \tag{9a}$$

$$v_0 = B(T_1, \mathrm{T}_2)\mathrm{e}^{i\omega_2 T_0} + \overline{B}(T_1, \mathrm{T}_2)\mathrm{e}^{-i\omega_2 T_0} \tag{9b}$$

where A and B are complex functions of T_1, T_2.

Substituting equation (9) into equation (7) as follows:

$$\left(D_0{}^2+\omega_1{}^2\right)\mathrm{u}_1=\left[-2i\omega_1 D_1 A-i\omega_1\widehat{\mu}_1 A+10\widehat{\alpha}_1\omega_1{}^2A^3\overline{A}^2\right.$$
$$+3\widehat{\alpha}_2\omega_1{}^2A^2\overline{A}-3\widehat{\alpha}_3A^2\overline{A}-10\widehat{\alpha}_4A^3\overline{A}^2$$

$$\left.-35\widehat{\alpha}_5A^4\overline{A}^3\right]e^{i\omega_1T_0}+(\widehat{k}_1B)e^{i\omega_2T_0}+\left(\frac{\widehat{F}}{2}\right)e^{i\Omega T_0}$$
$$+\left[5\widehat{\alpha}_1\omega_1{}^2A^4\overline{A}+\widehat{\alpha}_2\omega_1{}^2A^3\right.$$

$$\left.-\widehat{\alpha}_3A^3-5\widehat{\alpha}_4A^4\overline{A}-21\widehat{\alpha}_5A^5\overline{A}^2\right]e^{3i\omega_1T_0}$$
$$+\left[\widehat{\alpha}_1\omega_1{}^2A^5-\widehat{\alpha}_4A^5-7\widehat{\alpha}_5A^6\overline{A}\right]e^{5i\omega_1T_0}$$

$$-\left[\widehat{\alpha}_5A^7\right]e^{7i\omega_1T_0}+cc \tag{10a}$$

$$\left(D_0{}^2+\omega_2{}^2\right)\mathrm{v}_1=\left[-2i\omega_2D_1B-i\omega_2\widehat{\mu}_2B\right]e^{i\omega_2T_0}$$
$$+\left[\widehat{k}_2A\right]e^{i\omega_1T_0}+cc \tag{10b}$$

where cc refers to the complex conjugate to the prior terms. For obtaining a bounded solution, the secular terms must be deleted. The general solutions for equation (10) are obtained as:

$$u_1=M_1(T_1,T_2)e^{i\omega_2T_0}+M_2(T_1,T_2)e^{3i\omega_1T_0}+M_3(T_1,T_2)e^{5i\omega_1T_0}$$
$$+M_4(T_1,T_2)e^{i\Omega T_0}$$

$$+M_5(T_1,T_2)e^{7i\omega_1T_0}+cc \tag{11a}$$

$$v_1=M_6(T_1,T_2)e^{i\omega_1T_0}+cc \tag{11b}$$

where $M_s(\mathrm{s}=1,2,..,6)$ are complex functions into T_1,T_2 , which are defined in the Appendix.

Substituting equations 9 and 11 into equation (8), and after that eliminating the secular terms, the particular solutions of (ε^2) are acquired in the following:

$$u_2=N_1(T_1,T_2)e^{i\omega_2T_0}+N_2(T_1,T_2)e^{3i\omega_1T_0}+N_3(T_1,T_2)e^{5i\omega_1T_0}$$
$$+N_4(T_1,T_2)e^{7i\omega_1T_0}$$

$$+N_5(T_1,T_2)e^{9i\omega_1T_0}+N_6(T_1,T_2)e^{11i\omega_1T_0}+N_7(T_1,T_2)e^{13i\omega_1T_0}$$
$$+N_8(T_1,T_2)e^{i\Omega T_0}$$

$$+N_9(T_1,T_2)e^{i(\omega_2+2\omega_1)T_0}+N_{10}(T_1,T_2)e^{i(\omega_2-2\omega_1)T_0}$$
$$+N_{11}(T_1,T_2)e^{i(\omega_2+4\omega_1)T_0}$$

$$+N_{12}(T_1,T_2)e^{i(\omega_2-4\omega_1)T_0}+N_{13}(T_1,T_2)e^{i(\omega_2+6\omega_1)T_0}$$
$$+N_{14}(T_1,T_2)e^{i(\omega_2-6\omega_1)T_0}$$

$$+N_{15}(T_1,T_2)e^{i(\Omega+2\omega_1)T_0}+N_{16}(T_1,T_2)e^{i(\Omega-2\omega_1)T_0}$$
$$+N_{17}(T_1,T_2)e^{i(\Omega+4\omega_1)T_0}$$

$$+N_{18}(T_1,T_2)e^{i(\Omega-4\omega_1)T_0}+N_{19}(T_1,T_2)e^{i(\Omega+6\omega_1)T_0}$$
$$+N_{20}(T_1,T_2)e^{i(\Omega-6\omega_1)T_0}+cc \tag{12a}$$

$$v_2=N_{21}(T_1,T_2)e^{i\omega_1T_0}+N_{22}(T_1,T_2)e^{3i\omega_1T_0}$$
$$+N_{23}(T_1,T_2)e^{5i\omega_1T_0}$$
$$+N_{24}(T_1,T_2)e^{7i\omega_1T_0}$$

$$+N_{25}(T_1,T_2)e^{i\Omega T_0}+cc \tag{12b}$$

where $N_s(\mathrm{s}=1,2,....,31)$ are complex functions in T_1,T_2 , which are presented in the Apppendix.

3. Stability investigation

The simultaneous primary and internal resonance $(\Omega\cong\omega_1,\omega_2\cong\omega_1)$ are studied in this portion for obtaining the stability of this behavior system. So, we enter the detuning parameter σ_1 as

$$\Omega=\omega_1+\sigma_1=\omega_1+\varepsilon\widehat{\sigma}_1,\omega_2=\omega_1+\sigma_2=\omega_2+\varepsilon\widehat{\sigma}_2 \tag{13}$$

where σ_1 represents the nearness of Ω to ω_1 and σ_2 represents the nearness between ω_1, ω_2. Putting equation (13) in equation (10) to obtain the solvability conditions from the removed secular terms and then scaling each parameter back to its authentic value, we acquire

$$-2i\omega_1D_1A-i\omega_1\widehat{\mu}_1A+10\alpha_1\omega_1{}^2A^3\overline{A}^2+3\alpha_2\omega_1{}^2A^2\overline{A}$$
$$-3\alpha_3A^2\overline{A}-10\alpha_4A^3\overline{A}^2-35\alpha_5A^4\overline{A}^3$$

$$+\frac{F}{2}e^{i\sigma_1T_1}+K_1Be^{i\sigma_2T_1}=0 \tag{14a}$$

$$-2i\omega_2D_1B-i\omega_2\widehat{\mu}_2B+K_2Ae^{-i\sigma_2T_1}=0 \tag{14b}$$

Putting

$$\mathrm{A}=\left(\frac{a}{2}\right)e^{i\gamma_1(T_1)},B=\left(\frac{b}{2}\right)e^{i\gamma_2(T_1)} \tag{15}$$

where (a,b) and (γ_1,γ_2) are the steady-state amplitudes and phases for the microbeam system and the PPF controller, respectively.

Substituting equation (15) in equation (14) and then equating real and imaginary portions

$$\dot{a}=-\frac{\mu_1}{2}a+\frac{F}{2\omega_1}\sin\theta_1+\frac{k_1}{2\omega_1}\mathrm{b}\sin\theta_2 \tag{16a}$$

$$a\dot{\gamma}_1 = \frac{3}{8}\left(\frac{\alpha_3}{\omega_1} - \alpha_2\omega_1\right)a^3 + \frac{5}{16}\left(\frac{\alpha_4}{\omega_1} - \alpha_1\omega_1\right)\mathrm{a}^5 + \left(\frac{35\alpha_5}{128\omega_1}\right)\mathrm{a}^7 - \frac{F}{2\omega_1}\cos\theta_1 - \frac{k_1 b}{2\omega_1}\cos\theta_2 \tag{16b}$$

$$\dot{b} = -\frac{\mu_2}{2}b - \frac{k_2}{2\omega_2}a\sin\theta_2 \tag{17a}$$

$$b\dot{\gamma}_2 = -\frac{k_2}{2\omega_2}a\cos\theta_2 \tag{17b}$$

$$\text{where } \theta_1 = \sigma_1 t - \gamma_1 \Rightarrow \dot{\gamma}_1 = \sigma_1 - \dot{\theta}_1, \theta_2 = \sigma_2 t + \gamma_2 - \gamma_1 \Rightarrow \dot{\gamma}_2 = \sigma_1 - \sigma_2 + \dot{\theta}_2 - \dot{\theta}_1 \tag{18}$$

Substituting equation (18) in equations (16) and (17), we obtain the following:

$$\dot{a} = -\frac{\mu_1}{2}a + \frac{F}{2\omega_1}\sin\theta_1 + \frac{k_1}{2\omega_1}\mathrm{b}\sin\theta_2 \tag{19a}$$

$$a\dot{\theta}_1 = a\sigma_1 - \frac{3}{8}\left(\frac{\alpha_3}{\omega_1} - \alpha_2\omega_1\right)a^3 - \frac{5}{16}\left(\frac{\alpha_4}{\omega_1} - \alpha_1\omega_1\right)\mathrm{a}^5 - \left(\frac{35\alpha_5}{128\omega_1}\right)\mathrm{a}^7 + \frac{F}{2\omega_1}\cos\theta_1 + \frac{k_1 b}{2\omega_1}\cos\theta_2 \tag{19b}$$

$$\dot{b} = -\frac{\mu_2}{2}b - \frac{k_2}{2\omega_2}a\sin\theta_2 \tag{20a}$$

$$b\dot{\theta}_2 = b\sigma_2 - \frac{k_2}{2\omega_2}a\cos\theta_2 - \frac{3}{8}\left(\frac{\alpha_3}{\omega_1} - \alpha_2\omega_1\right)\mathrm{b}a^2 - \frac{5}{16}\left(\frac{\alpha_4}{\omega_1} - \alpha_1\omega_1\right)\mathrm{b}a^4 - \left(\frac{35\alpha_5}{128\omega_1}\right)\mathrm{b}a^6 + \frac{F}{2\omega_1 a}\mathrm{b}\cos\theta_1 + \frac{k_1 b^2}{2\omega_1 a}\cos\theta_2 \tag{20b}$$

To reach the steady-state solutions of the microbeam system and the PPF controller by setting $(\dot{\mathrm{a}} = \dot{b} = \dot{\theta}_1 = \dot{\theta}_2 = 0)$ in equations (19) and (20) yields

$$\frac{\mu_1}{2}a = \frac{F}{2\omega_1}\sin\theta_1 + \frac{k_1}{2\omega_1}\mathrm{b}\sin\theta_2 \tag{21a}$$

$$\left[a\sigma_1 - \frac{3}{8}\left(\frac{\alpha_3}{\omega_1} - \alpha_2\omega_1\right)a^3 - \frac{5}{16}\left(\frac{\alpha_4}{\omega_1} - \alpha_1\omega_1\right)\mathrm{a}^5 - \left(\frac{35\alpha_5}{128\omega_1}\right)\mathrm{a}^7\right] = -\frac{F}{2\omega_1}\cos\theta_1 - \frac{k_1 b}{2\omega_1}\cos\theta_2 \tag{21b}$$

$$\frac{\mu_2}{2}b = -\frac{k_2}{2\omega_2}a\sin\theta_2 \tag{22a}$$

$$b(\sigma_1 - \sigma_2) = -\frac{k_2}{2\omega_2}a\cos\theta_2 \tag{22b}$$

Using equation (21) and (22), we get two cases of frequency response equations (FRE).

Case (1): (microbeam system in the absence of control) in which $(a \neq 0,\ b = 0)$, the frequency response equation is acquired from equations (21) and (22) as follows:

$$\left(\sigma_1 - \frac{3}{8}\left(\frac{\alpha_3}{\omega_1} - \alpha_2\omega_1\right)a^3 - \frac{5}{16}\left(\frac{\alpha_4}{\omega_1} - \alpha_1\omega_1\right)\mathrm{a}^5 - \left(\frac{35\alpha_5}{128\omega_1}\right)\mathrm{a}^7\right)^2 + \frac{{\mu_1}^2}{4}a^2 - \frac{F^2}{4{\omega_1}^2} = 0 \tag{23}$$

Case (2): (microbeam system in the existence of control) in which $(a \neq 0, b \neq 0)$ the frequency response equation is obtained from equations (21) and (22) as follows:

$$b^2\left[(\sigma_1 - \sigma_2)^2 + \frac{{\mu_2}^2}{4}\right] - \frac{{k_2}^2}{4{\omega_2}^2}a^2 = 0 \tag{24a}$$

$$\left(a\sigma_1 - \frac{3}{8}\left(\frac{\alpha_3}{\omega_1} - \alpha_2\omega_1\right)a^3 - \frac{5}{16}\left(\frac{\alpha_4}{\omega_1} - \alpha_1\omega_1\right)\mathrm{a}^5 - \left(\frac{35\alpha_5}{128\omega_1}\right)\mathrm{a}^7\right)^2 + \frac{{\mu_1}^2 a^2}{4} - \frac{F^2}{4{\omega_1}^2} - \frac{{k_1}^2 b^2}{4{\omega_1}^2} - \frac{F k_1 b}{2{\omega_1}^2} = 0 \tag{24b}$$

For investigating the nonlinear solution's stability, we may put

$$a = a_0 + a_1, b = b_0 + b_1, \theta_n = \theta_{n0} + \theta_{n1}, (n = 1, 2) \tag{25}$$

where $a_0, \mathrm{b}_0, \theta_{n0}$ are the solutions for equations (21) and (22). Putting equation (25) into equations (19) and (20), with the preservation of only linear terms into a_1, b_1 and θ_{n1}, we obtain

$$\dot{a}_1 = -\left(\frac{\mu_1}{2}\right)a_1 + \left(\frac{F}{2\omega_1}\cos\theta_{10}\right)\theta_{11} + \left(\frac{k_1}{2\omega_1}\sin\theta_{20}\right)b_1 + \left(\frac{k_1 b_0}{2\omega_1}\cos\theta_{20}\right)\theta_{21} \tag{26a}$$

$$\dot{\theta}_{11} = \left(\frac{\sigma_1}{a_0} - \frac{9a_0}{8}\left(\frac{\alpha_3}{\omega_1} - \alpha_2\omega_1\right) - \frac{25{a_0}^3}{16}\left(\frac{\alpha_4}{\omega_1} - \alpha_1\omega_1\right) - \frac{245{a_0}^5}{128\omega_1}\right)a_1 - \left(\frac{F}{2\omega_1 a_0}\sin\theta_{10}\right)\theta_{11} + \left(\frac{k_1}{2\omega_1 a_0}\cos\theta_{20}\right)b_1 - \left(\frac{k_1 b_0}{2\omega_1 a_0}\sin\theta_{20}\right)\theta_{21} \tag{26b}$$

$$\dot{b}_1 = -\left(\frac{k_2}{2\omega_2}\sin\theta_{20}\right)a_1 - \left(\frac{\mu_2}{2}\right)b_1 - \left(\frac{k_2 a_0}{2\omega_2}\cos\theta_{20}\right)\theta_{21} \tag{27a}$$

$$\dot{\theta}_{21} = \left(\frac{\sigma_2}{a_0} - \frac{9}{8}\left(\frac{\alpha_3}{\omega_1} - \alpha_2\omega_1\right)a_0 - \frac{25}{16}\left(\frac{\alpha_4}{\omega_1} - \alpha_1\omega_1\right){a_0}^3 - \frac{245\alpha_5}{128\omega_1}{a_0}^5 - \frac{k_2}{\omega_2 b_0}\cos\theta_{20}\right)a_1 - \left(\frac{F\sin\theta_{10}}{2\omega_1 a_0}\right)\theta_{11} + \left(\frac{\sigma_2}{b_0} - \frac{3}{8b_0}\left(\frac{\alpha_3}{\omega_1} - \alpha_2\omega_1\right){a_0}^2 - \frac{5}{16b_0}\left(\frac{\alpha_4}{\omega_1} - \alpha_1\omega_1\right){a_0}^4 - \frac{35\alpha_5}{128b_0\omega_1}{a_0}^6 + \frac{k_1}{\omega_1 a_0}\cos\theta_{20} + \frac{F\cos\theta_{10}}{2\omega_1 a_0 b_0}\right)b_1 + \left(\frac{k_2 a_0}{2\omega_2 b_0}\sin\theta_{20} - \frac{k_1 b_0}{2\omega_1 a_0}\sin\theta_{20}\right)\theta_{21} \tag{27b}$$

The eigenvalues for equations (26) and (27) are acquired from the following:

$$\lambda^4 + g_1\lambda^3 + g_2\lambda^2 + g_3\lambda + g_4 = 0 \tag{28}$$

where g_1, g_2, g_3, g_4 are the coefficients of equations (26) and (27). As a result, the nonlinear solution's stability is obtained if the real part of the eigenvalues is negative. Else, it is unstable. With the assistance of the Routh-Hurwitz standard, the necessary and enough conditions that the roots of equation (28), having negative real portions are

$$g_1 > 0, g_1 g_2 - g_3 > 0, g_3(g_1 g_2 - g_3) - {g_1}^2 g_4 > 0, g_4 > 0 \tag{29}$$

4. Results and discussions

In this section, the Runge-Kutta fourth-order technique utilizing Matlab7.7 (R2014) and Maple16 software is applied to discuss the numerical solutions of the considered system of equations (1) and (2) before and after adding the control at the following parameter values:

$$\mu_1 = 0.05, \alpha_1 = 0.1319, \alpha_2 = 0.3338, \alpha_3 = 0.3331, \alpha_4 = 0.1299, \alpha_5 = 0.2, F = 1.5$$

$$\Omega = 2.4, \omega_1 = 2.4, \omega_2 = 2.4, \mu_2 = 0.005, \mathrm{K}_1 = 2.4, \mathrm{K}_2 = 1.2$$

Figure 2 shows the time history and phase plane of the uncontrolled microbeam system at the case ($\Omega \cong \omega_1,\ \omega_2 \cong \omega_1$). Meantime in this figure, we noticed that the microbeam system amplitude is nearly 67.5 from the excitation forcing F, and the phase plane shows stability accompanied by several limit cycles. Figure 3 displays the controlled microbeam system and the PPF controller and their phase planes at the resonance $\Omega \cong \omega_1, \omega_2 \cong \omega_1$ state. In this figure, the PPF controller minimized the vibrations to about 0.006247 as shown in Fig. 3. So, the effectiveness of this control is E_a (E_a = uncontrolled microbeam system amplitude/controlled microbeam system amplitude) is about 162, which means the PPF controller minimized the amplitude for the microbeam system by about 99.4%.

4.1. Effects of various parameters on the microbeam system and the controller

The frequency response equations that are given in equations (23) and (24) are solved utilizing Maple (16) and Matlab7.7 (R2014) software as illustrated in the following figures. Figure 4 illustrates the response curves for uncontrolled microbeam system in equation (23) of Case (1) ($a \neq 0, b = 0$) under various values of the excitation forcing amplitude F. It can be noticed that the amplitude for the microbeam system is directly proportional to the excitation forcing amplitude F.

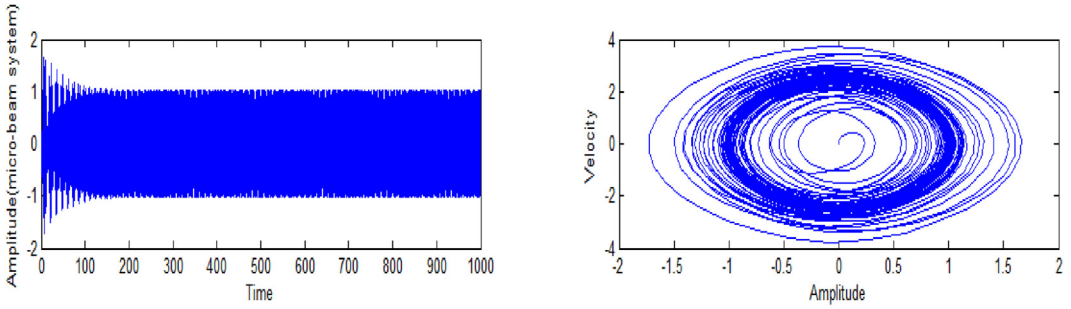

Fig. 2. Uncontrolled microbeam system at the case $\Omega \cong \omega_1, \omega_2 \cong \omega_1$.

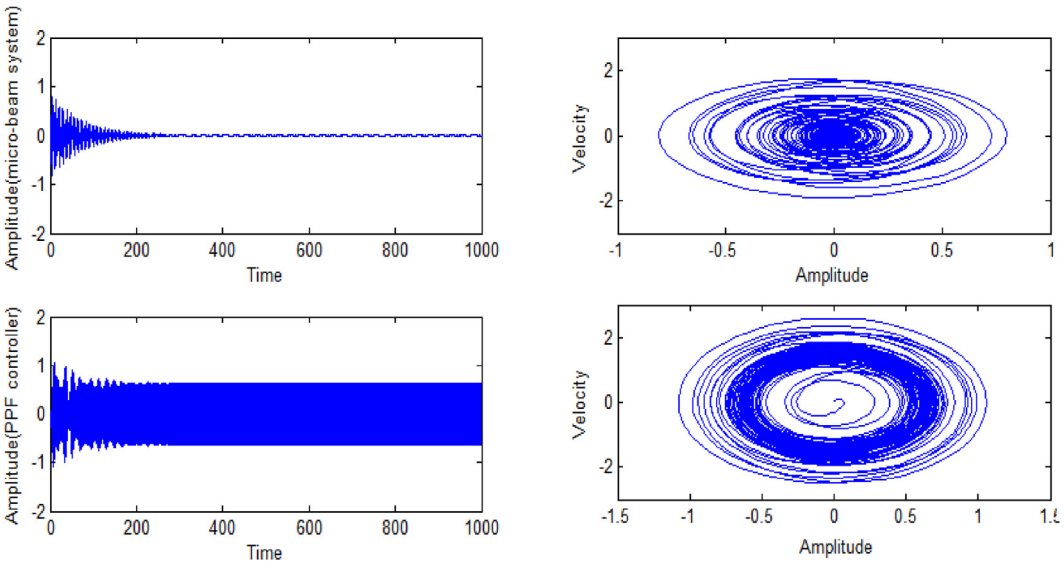

Fig. 3. Controlled microbeam system and the PPF controller at the case $\Omega \cong \omega_1, \omega_2 \cong \omega_1$.

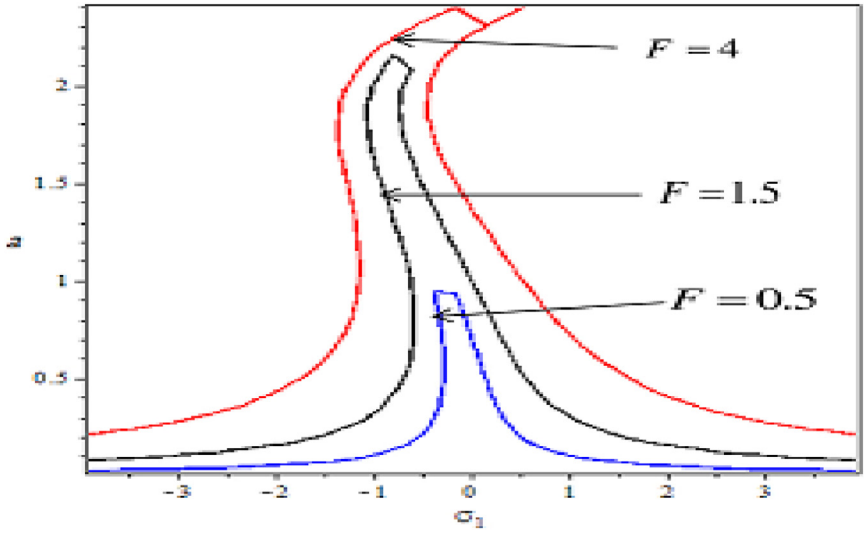

Fig. 4. Effect of the excitation forcing amplitude F in the absence of the control.

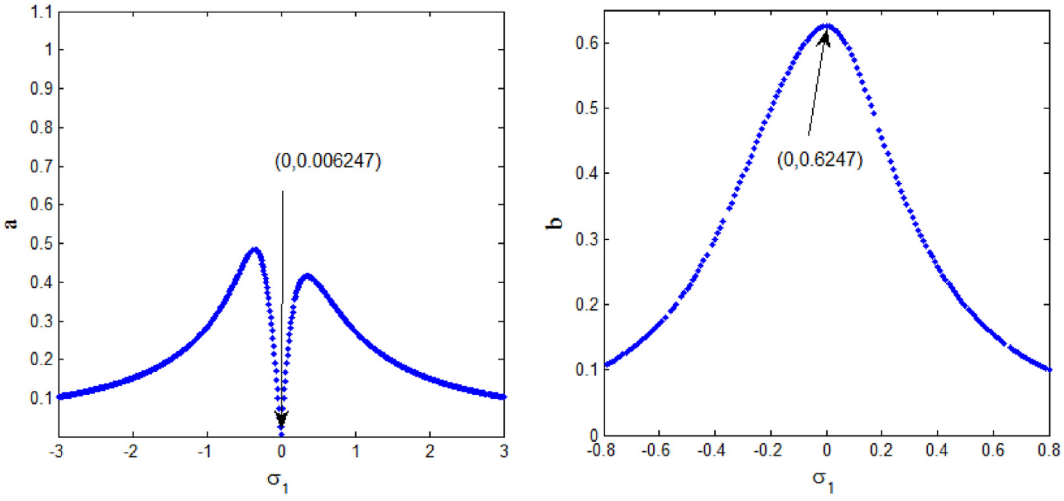

Fig. 5. Frequency response curves of the controlled microbeam system amplitudes. (a, microbeam and b, PPF controller) against σ_1 *of Case (2)* ($a \neq 0$, $b \neq 0$).

Moreover, the response curve is bent to the right which leads to a hard spring, and the jump phenomena appears for increasing values of the excitation forcing amplitude F. Figure 5 illustrates the frequency response curves (FRC), which is given in equation (24) of Case (2) $(a \neq 0, b \neq 0)$ of the controlled microbeam system amplitudes, which consist of the microbeam system amplitude

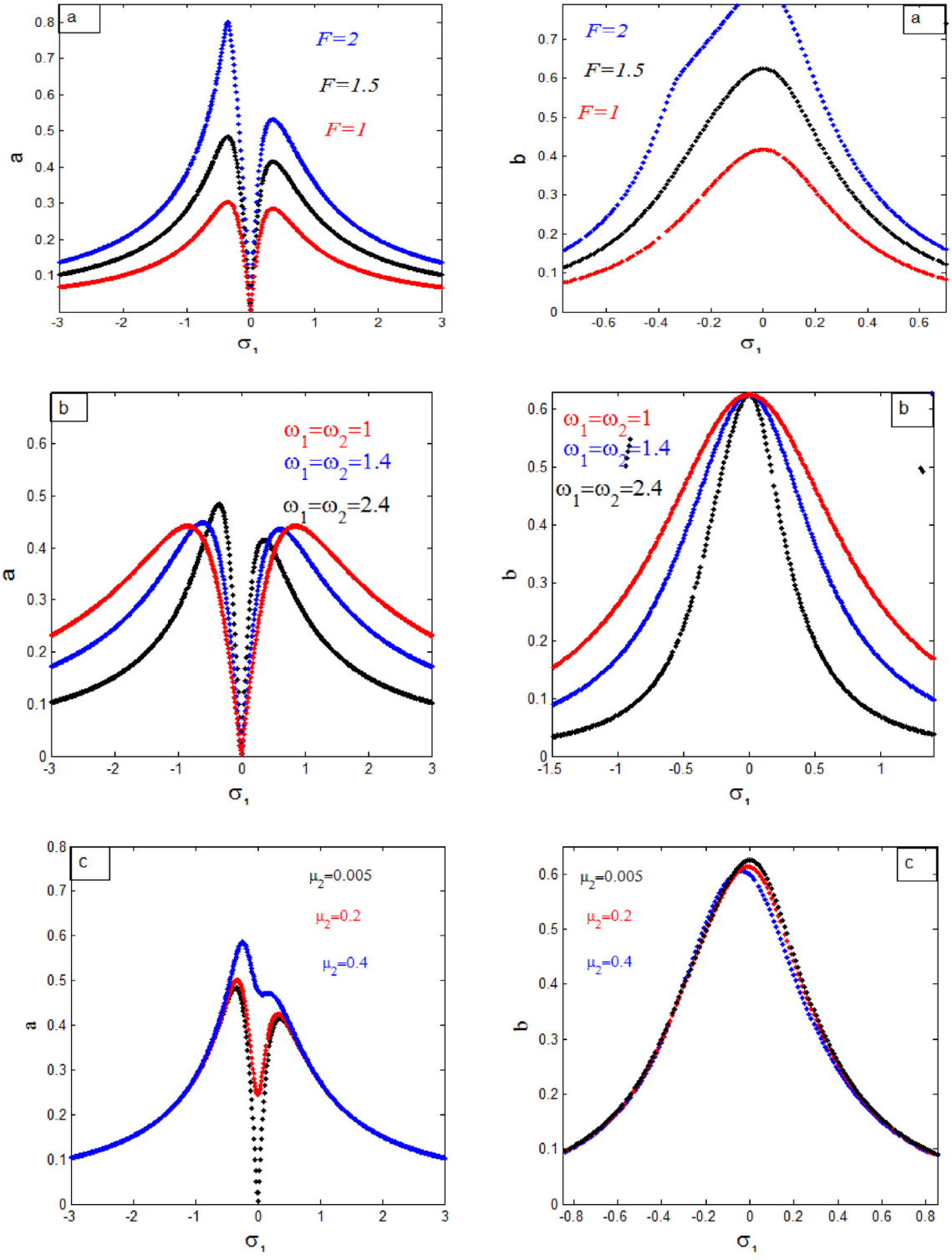

Fig. 6 Effects of different parameters on the frequency response curves of the controlled microbeam system amplitudes (a, b).

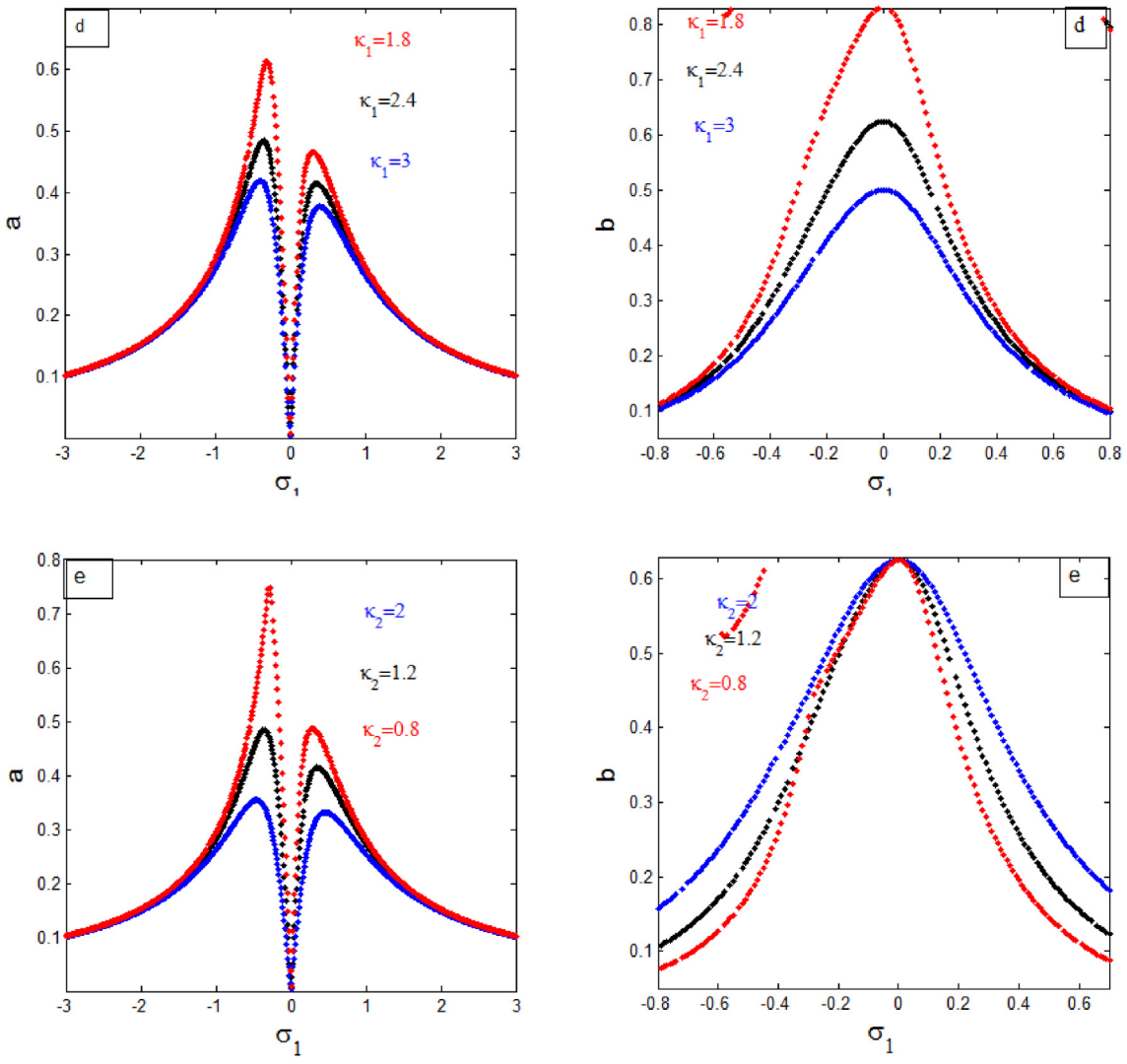

Fig. 6 (Continued).

(a) and the PPF controller amplitude (b) versus the detuning parameter σ_1 with the self same parameter values, where stable solutions are clarified by solid lines, while unstable solutions are distinguished by dashed lines. From this figure, we can sight that the amplitudes a = 0.006247and b = 0.6247. These values are very close to the amplitudes of the microbeam system (u) and the controller (v) that are obtained in Fig. 3. The effects of different parameters are discussed in Fig. 6. Figure 6a and b demonstrate the controlled microbeam system amplitudes (a, b) in are directly proportional to the excitation forcing amplitude F, but inversely proportional to the natural frequency ω_1. In addition the instability zones become more extensive for increasing or decreasing of the excitation forcing amplitude F and natural frequency ω_1, respectively. The effect of the damping coefficient μ_2 on the controlled microbeam system amplitudes (a, b) is shown in Fig. 6c. It can be seen that for big values of μ_2 of the microbeam amplitude (a) the system's solution becomes stable and the instability zones are vanished and the curve of the PPF controller amplitude (b) is decreased and became more narrow. Figure 6d indicates that the controlled microbeam system amplitudes (a, b) are inversely proportional to the control signal gain k_1, which is in good agreement with Fig. 8. Figure 6e shows the increase of the feedback signal gain k_2 on the controlled microbeam system amplitudes (a, b). It is noticeable for increasing the values of k_2 leading to a decrease in the amplitude (a) and increasing amplitude (b) which is good agreement with Fig. 9.

The effects of the detuning parameter σ_2 on the response curves are illustrated in Fig. 7. Figure 7a shows that the controlled microbeam system amplitudes (a, b) arrive at lesser values at $\sigma_2 = 0$, which emphasized that the controller is capable to minimize the oscillations to less values. Through that figure, we noticed that the amplitudes a = 0.006247 and b = 0.6247; these values are very close to the amplitudes of the controlled microbeam system amplitudes (a, b) as shown in Fig. 3 and Fig. 5. The amplitude (a) of the microbeam system are inversely proportional to the damping coefficient μ_2, nonlinear parameters α_1, α_2, and the natural frequencies ω_1, ω_2 as demonstrated in Fig. 7b, d, e, and g. For increasing values of the excitation forcing amplitude F and the nonlinear parameter α_3, the amplitude (a) of the microbeam system is increased as displayed in Fig. 7c and f. Figures 8 and 9 illustrate the effects of the control and feedback signal gains k_1, k_2 of response curves at $\sigma_1 = \sigma_2 = 0$, respectively. We noticed that the stability zones are increasing for decreasing values of k_1, k_2 or increasing for growing values of k_2 of the controller amplitude (b).

(a) FRC of the controlled the microbeam system amplitudes of Case (2) $(a \neq 0, b \neq 0)$.

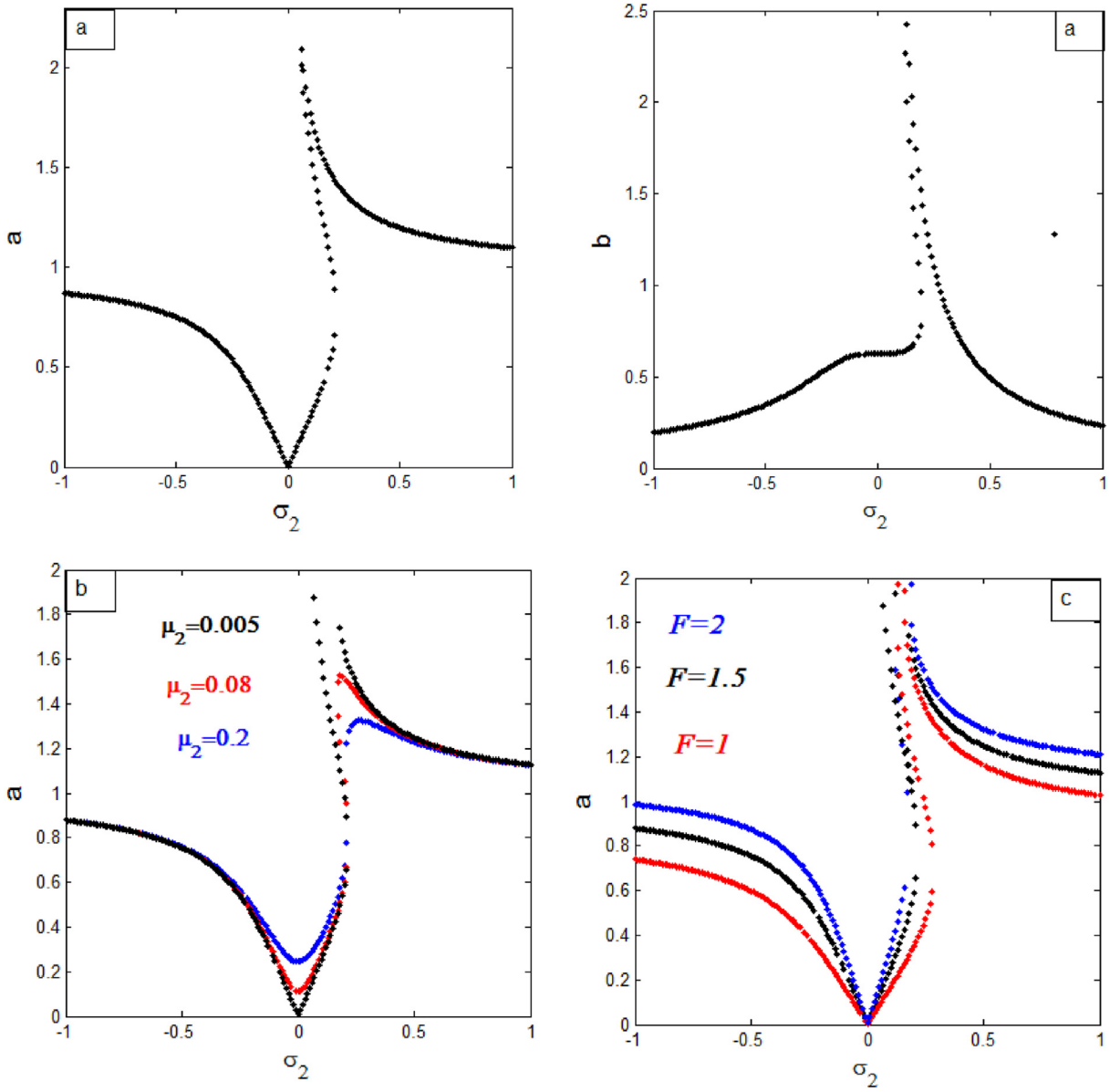

Fig. 7 Effects of different parameters on the FRC((a) microbeam) versus σ_2.

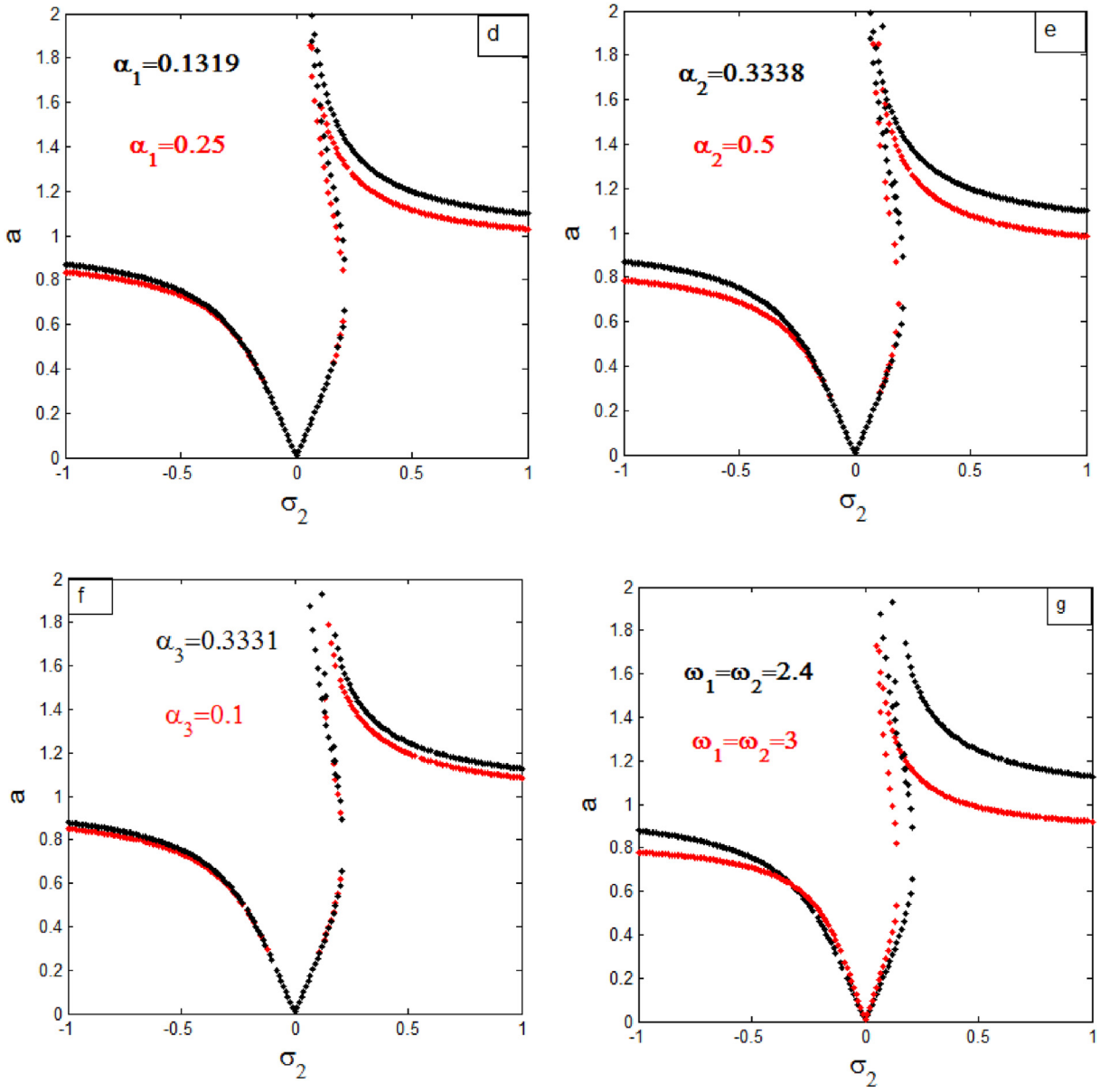

Fig. 7 (Continued).

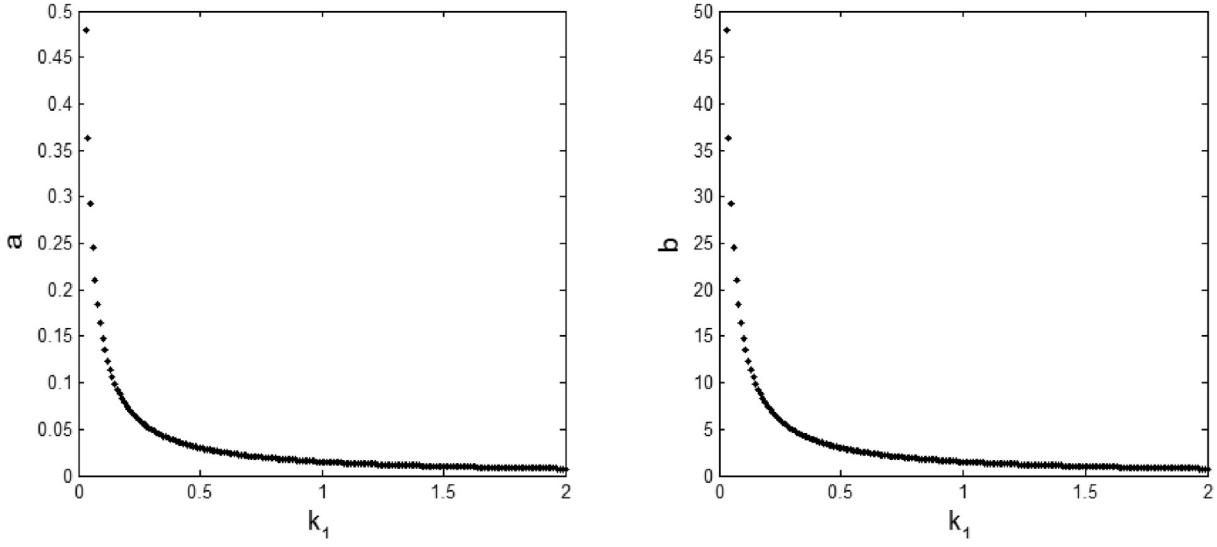

Fig. 8. The response curves amplitudes versus the control gain k_1 at $\sigma_1 = \sigma_2 = 0$.

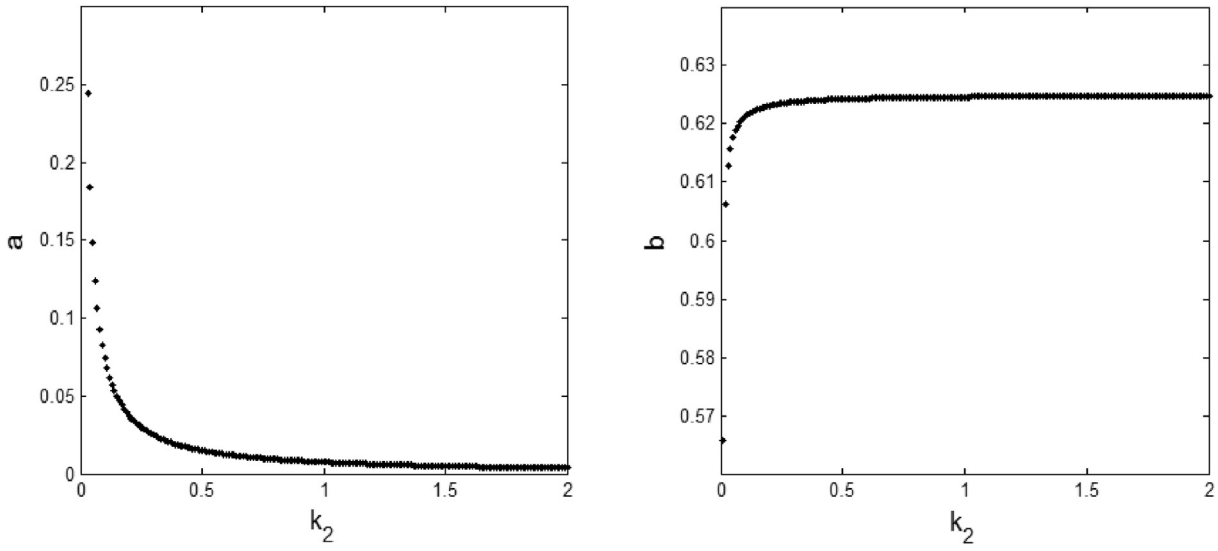

Fig. 9. Response curve amplitudes versus the control gain k_2 at $\sigma_1 = \sigma_2 = 0$.

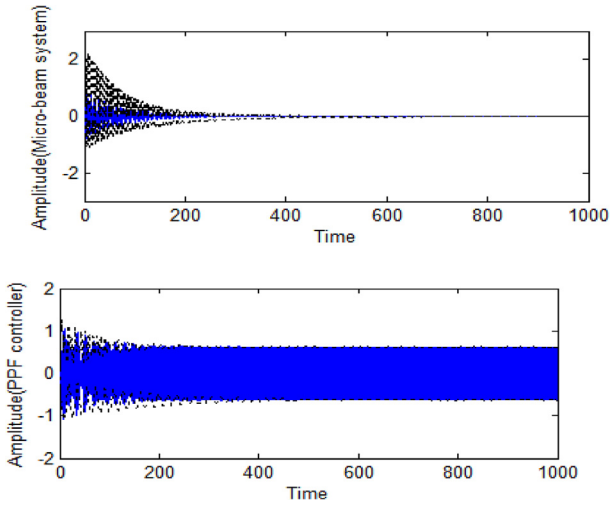

Fig. 10. Time history of analytical solution (black dashed lines) and numerical simulation (blue solid lines).

$(a \neq 0, b \neq 0)$ (a, microbeam and b, controller) against σ_2.

4.2. Comparison with numerical simulation

In this subsection, we compared the analytical solution presented using MSP in equations (16) and (17), and the numerical simulation induced by the Runge-Kutta method (RKM) in equations (1) and (2). Figure 10 shows the closeness between the analytical solution (black dashed lines) and the numerical simulation (blue solid lines).

5. Conclusions

The PPF controller was used in this study to minimize the vibrations of a clamped–clamped microbeam system. The MSP technique is used for solving these equations analytically of the controlled microbeam system. Also, the stability behavior of the controlled microbeam system at the simultaneous resonance cases using the frequency response equations was discussed. The whole system was examined numerically for different parameters that affected the frequency response curves before and after the control. According to the aforementioned study, we might deduce that.

(1) With the aid of the PPF controller, the uncontrolled microbeam system amplitude is minimized to 99.4 from its value.
(2) The controller's efficiency E_a was about 162 as displayed in Fig. 3.
(3) The controlled microbeam system amplitudes (a, b) are directly proportional to the excitation forcing amplitude F, but inversely proportional to the natural frequency ω_1. In addition the instability zones become more extensive for increasing or decreasing the excitation forcing amplitude F and the natural frequency ω_1, respectively.
(4) The controlled microbeam system amplitudes (a, b) arrive at lesser values at $\sigma_2 = 0$, which emphasized that the controller is capable to minimize the oscillations to lesser values.

(5) The stability zones are increasing for decreasing values of k_1, k_2 or increasing for growing values of k_2 for the PPF controller amplitude (b) as shown in Figs. 8 and 9.
(6) The study demonstrates that all foretelling derived from the analytical solutions and numerical solutions agree fairly together well as shown in Fig. 10.

Funding

The authors received no financial support for the research, authorship, and/or publication of this article.

Conflicts of interest

The authors declared no potential conflicts of interest with respect to the research, authorship, and/or publication of this article.

Acknowledgments

The author would like to thank department of mathematics, faculty of Science(Boys), Al-Azhar university, for supporting this study.

Appendix

Coefficients of equation (11)

$$M_1=\frac{\widehat{k}_1 B}{{\omega_1}^2-{\omega_2}^2}, M_2=\frac{-\left[5\widehat{\alpha}_1{\omega_1}^2A^4\overline{A}+\widehat{\alpha}_2{\omega_1}^2A^3-\widehat{\alpha}_3A^3-5\widehat{\alpha}_4A^4\overline{A}-21\widehat{\alpha}_5A^5\overline{A}^2\right]}{8{\omega_1}^2}$$

$$M_3=\frac{-\left[\widehat{\alpha}_1{\omega_1}^2A^5-\widehat{\alpha}_4A^5-7\widehat{\alpha}_5A^6\overline{A}\right]}{24{\omega_1}^2}, M_4=\frac{\widehat{F}}{2\left({\omega_1}^2-\Omega^2\right)}, M_5=\frac{\left[\widehat{\alpha}_5A^7\right]}{48{\omega_1}^2}, M_6=\frac{[\widehat{k}_2A]}{{\omega_2}^2-{\omega_1}^2}$$

Coefficients of equation (12*a*)

$$N_1=\frac{-2i\omega_2(\mathrm{D}_1M_1)-i\widehat{\mu}_1\omega_2M_1-6\widehat{\alpha}_1\omega_2{}^2A^2\overline{A}^2M_1-24\widehat{\alpha}_1{\omega_1}^2A^2\overline{A}^2M_1-2\widehat{\alpha}_2A\overline{A}M_1({\omega_2}^2+2{\omega_1}^2)}{{\omega_1}^2-{\omega_2}^2}$$
$$+\frac{6\widehat{\alpha}_3A\overline{A}M_1+30\widehat{\alpha}_4A^2\overline{A}^2M_1+140\widehat{\alpha}_5A^3\overline{A}^3M_1}{{\omega_1}^2-{\omega_2}^2}$$

$$N_2=\frac{-6i\omega_1(\mathrm{D}_1M_2)-3i\widehat{\mu}_1\omega_1M_2-\widehat{\alpha}_1{\omega_1}^2\left(53\overline{A}^4M_5+78A^2\overline{A}^2M_2+112A\overline{A}^3M_3\right)}{-8{\omega_1}^2}$$

$$+\frac{\widehat{\alpha}_1\left[-2i\omega_1(\mathrm{D}_1\overline{A})\mathrm{A}^4+8i\omega_1(\mathrm{D}_1A)\mathrm{A}\overline{\mathrm{A}}^3\right]}{-8{\omega_1}^2}$$

$$+\frac{\widehat{\alpha}_2\left[2i\omega_1(\mathrm{D}_1A)\mathrm{A}^2-22\omega_1{}^2\mathrm{A}\overline{\mathrm{A}}M_2-27\omega_1{}^2\overline{A}^2M_3\right]}{-8{\omega_1}^2}$$

$$+\frac{\widehat{\alpha}_3\left(3\overline{A}^2M_3+6A\overline{A}M_2\right)+\widehat{\alpha}_4\left(5\overline{A}_4M_5+20A\overline{A}^3M_3+30A^2\overline{A}^2M_2\right)+\widehat{\alpha}_5\left(7\overline{A}^6\overline{M}_2\right)}{-8{\omega_1}^2}$$

$$+\frac{\widehat{\alpha}_5\left(42A\overline{A}^5M_5+105\overline{A}^4A^2M_3+140A^3\overline{A}^3M_2\right)}{-8{\omega_1}^2}$$

$$N_3=\frac{-10i\omega_1(\mathrm{D}_1M_3)-5i\widehat{\mu}_1\omega_1M_3-\widehat{\alpha}_1{\omega_1}^2\left(212\mathrm{A}\overline{A}^3M_5+174A^2\overline{A}^2M_3+52A^3\overline{A}M_2\right)}{-24{\omega_1}^2}$$

$$+\frac{\widehat{\alpha}_1\left[2i\omega_1(\mathrm{D}_1\mathrm{A})\mathrm{A}^4\right]-\widehat{\alpha}_2{\omega_1}^2\left[11\mathrm{A}^2M_2+54\mathrm{A}\overline{A}M_3+51\overline{A}^2M_5\right]}{-24{\omega_1}^2}$$

$$+\frac{\widehat{\alpha}_3\left[3\mathrm{A}^2M_2+6\mathrm{A}\overline{A}M_3+3\overline{A}^2M_5\right]+\widehat{\alpha}_4\left[20\mathrm{A}^3\overline{A}M_2+20\mathrm{A}\overline{A}^3M_5+30A^2\overline{A}^2M_3\right]}{-24{\omega_1}^2}$$

$$+\frac{\widehat{\alpha}_5\left[105\mathrm{A}^4\overline{A}^2M_2+105\mathrm{A}^2\overline{A}^4M_5+140A^3\overline{A}^3M_3\right]}{-24{\omega_1}^2}$$

$$N_4=\frac{-14i\omega_1(\mathrm{D}_1M_5)-7i\widehat{\mu}_1\omega_1M_5-\widehat{\alpha}_1{\omega_1}^2\left(13\mathrm{A}^4M_2+318A^2\overline{A}^2M_5+112A^3\overline{A}M_3\right)}{-48{\omega_1}^2}$$

$$+\frac{-\widehat{\alpha}_2{\omega_1}^2\left[27\mathrm{A}^2M_3+102\mathrm{A}\overline{A}M_5\right]+\widehat{\alpha}_3\left[3A^2M_3+6A\overline{A}M_5\right]}{-48{\omega_1}^2}$$

$$+\frac{\widehat{\alpha}_4\left[5\mathrm{A}^4M_2+20\mathrm{A}^3\overline{A}M_3+30\mathrm{A}^2\overline{\mathrm{A}}^2\mathrm{M}_5\right]+\widehat{\alpha}_5\left[42A^5\overline{A}M_2+105A^4\overline{A}^2M_3+140\mathrm{A}^3\overline{\mathrm{A}}^3\mathrm{M}_5\right]}{-48{\omega_1}^2}$$

$$N_5=\frac{-\widehat{\alpha}_1{\omega_1}^2\left(25\mathrm{A}^4M_3+212A^3\overline{A}M_5\right)-51\widehat{\alpha}_2{\omega_1}^2A^2M_5+3\widehat{\alpha}_3A^2M_5}{-80{\omega_1}^2}$$

$$+\frac{\widehat{\alpha}_4\left(5\mathrm{A}^4M_3+20A^3\overline{A}M_5\right)+\widehat{\alpha}_5\left(7A^6M_2+42A^5\overline{A}M_3+105A^4\overline{A}^2M_5\right)}{-80{\omega_1}^2}$$

$$N_6=\frac{-\widehat{\alpha}_1{\omega_1}^2\left(53\mathrm{A}^4M_5\right)-5\widehat{\alpha}_4A^4M_5+\widehat{\alpha}_5\left(7A^6M_3+42A^5\overline{A}M_5\right)}{-120{\omega_1}^2},N_7=\frac{7\widehat{\alpha}_5A^6M_5}{-168{\omega_1}^2}$$

$$N_8=\frac{-2i\Omega(\mathrm{D}_1M_4)-i\widehat{\mu}_1\Omega M_4-\widehat{\alpha}_1A^2\overline{A}^2M_4\left(6\Omega^2+12{\omega_1}^2\right)-2\widehat{\alpha}_2A\overline{A}M_4\left(\Omega^2+2{\omega_1}^2\right)}{{\omega_1}^2-\Omega^2}$$

$$+\frac{6\widehat{\alpha}_3A\overline{A}M_4+30\widehat{\alpha}_4A^2\overline{A}^2M_4+140\widehat{\alpha}_5A^3\overline{A}^3M_4}{{\omega_1}^2-\Omega^2}$$

$$N_9=\frac{-4\widehat{\alpha}_1A^3\overline{A}M_1({\omega_2}^2+4{\omega_1}^2)-\widehat{\alpha}_2A^2M_1({\omega_2}^2+2{\omega_1}^2)+3\widehat{\alpha}_3A^2M_1+\widehat{\alpha}_4\left(20A^3\overline{A}M_1\right)+\widehat{\alpha}_5\left(105A^4\overline{A}^2M_1\right)}{{\omega_1}^2-\left(\omega_2+2\omega_1\right)^2}$$

$$N_{10}=\frac{-4\widehat{\alpha}_1A\overline{A}^3M_1({\omega_2}^2+4{\omega_1}^2)-\widehat{\alpha}_2\overline{A}^2M_1({\omega_2}^2+2{\omega_1}^2)+3\widehat{\alpha}_3\overline{A}^2M_1+\widehat{\alpha}_4\left(20A\overline{A}^3M_1\right)+\widehat{\alpha}_5\left(105A^2\overline{A}^4M_1\right)}{{\omega_1}^2-\left(\omega_2-2\omega_1\right)^2}$$

$$N_{11}=\frac{-\widehat{\alpha}_1A^4M_1({\omega_2}^2+4{\omega_1}^2)+\widehat{\alpha}_4\left(5A^4M_1\right)+\widehat{\alpha}_5\left(42A^5\overline{A}M_1\right)}{{\omega_1}^2-\left(\omega_2+4\omega_1\right)^2}$$

$$N_{12}=\frac{-\widehat{\alpha}_1\overline{A}^4M_1({\omega_2}^2+4{\omega_1}^2)+\widehat{\alpha}_4\left(5\overline{A}^4M_1\right)+\widehat{\alpha}_5\left(42A\overline{A}^5M_1\right)}{{\omega_1}^2-\left(\omega_2-4\omega_1\right)^2}$$

$$N_{13}=\frac{7\widehat{\alpha}_5A^6M_1}{{\omega_1}^2-\left(\omega_2+6\omega_1\right)^2},N_{14}=\frac{7\widehat{\alpha}_5\overline{A}^6M_1}{{\omega_1}^2-\left(\omega_2-6\omega_1\right)^2}$$

$$N_{15}=\frac{-4\widehat{\alpha}_1A^3\overline{A}M_4\left(\Omega^2+4{\omega_1}^2\right)+3\widehat{\alpha}_3A^2M_4+20\widehat{\alpha}_4A^3\overline{A}M_4+105\widehat{\alpha}_5A^4\overline{A}^2M_4}{{\omega_1}^2-\left(\Omega+2\omega_1\right)^2}$$

$$N_{16}=\frac{-4\widehat{\alpha}_1 A\overline{A}^3 M_4\left(\Omega^2+4{\omega_1}^2\right)+3\widehat{\alpha}_3\overline{A}^2 M_4+20\widehat{\alpha}_4 A\overline{A}^3 M_4+105\widehat{\alpha}_5 A^2\overline{A}^4 M_4}{{\omega_1}^2-\left(\Omega-2\omega_1\right)^2}$$

$$N_{17}=\frac{-4\widehat{\alpha}_1 A^4\Omega^2 M_4+5\widehat{\alpha}_4 A^4 M_4+42\widehat{\alpha}_5 A^5\overline{A} M_4}{{\omega_1}^2-\left(\Omega+4\omega_1\right)^2}, N_{18}=\frac{-4\widehat{\alpha}_1\overline{A}^4\Omega^2 M_4+5\widehat{\alpha}_4\overline{A}^4 M_4+42\widehat{\alpha}_5 A\overline{A}^5 M_4}{{\omega_1}^2-\left(\Omega-4\omega_1\right)^2}$$

$$N_{19}=\frac{7\widehat{\alpha}_5 A^6 M_4}{{\omega_1}^2-\left(\Omega+6\omega_1\right)^2}, N_{20}=\frac{7\widehat{\alpha}_5\overline{A}^6 M_4}{{\omega_1}^2-\left(\Omega-6\omega_1\right)^2}$$

Coefficients of equation (12b)

$$N_{21}=\frac{-2i\omega_1(D_1E_6)-i\mu_2\omega_1 E_6}{{\omega_2}^2-{\omega_1}^2}, N_{22}=\frac{\widehat{k}_2 E_2}{{\omega_2}^2-9{\omega_1}^2}, N_{23}=\frac{\widehat{k}_2 E_3}{{\omega_2}^2-25{\omega_1}^2}$$

$$N_{24}=\frac{\widehat{k}_2 E_5}{{\omega_2}^2-49{\omega_1}^2}, N_{25}=\frac{\widehat{k}_2 E_3}{{\omega_2}^2-\Omega^2}$$

References

[1] Ekici H, Boyaci H. Effects of non-ideal boundary conditions on vibrations of microbeams. J Vib Control 2007;13:1369−78.

[2] Nayfeh AH, Younis MI. Dynamics of MEMS resonators under super-harmonic and sub-harmonic excitations. J Micromech Microeng 2005;15:1840−7.

[3] Younis MI, Nayfeh AH. A study of the nonlinear response of a resonant micro-beam to an electric actuation. Nonlinear Dynam 2003;31:91−117.

[4] Elnaggar AM, Bassiouny AF, Mosa GA. Harmonic and subharmonic resonance of MEMS subjected to weakly nonlinear parametric and external excitations. Int J Appl Math Res 2013;2:252−63.

[5] Younesian D, Sadri M, Esmailzadeh E. Primary and secondary resonance analyses of clamped−clamped microbeams. Nonlinear Dynam 2014;76:1867−84.

[6] Amer YA, El-Sayed AT, El-Bhrawy FT. Torsional vibration reduction for rolling mill's main drive system via negative velocity feedback under parametric excitation. J Mech Sci Technol 2015;29:1581−9.

[7] Kandil A, El-Gohary HA. Suppressing the nonlinear vibrations of a compressor blade via a nonlinear saturation control. J Vib Control 2016;24:1−17.

[8] El-Sayed AT, Bauomy HS. Outcome of special vibration controller techniques linked to a cracked beam. Appl Math Modell 2018;63:266−87.

[9] Hamed YS, Sayed M, Alshehri AA. Active vibration suppression of a nonlinear electromechanical oscillator system with simultaneous resonance. J Vibroeng 2018;20:42−61.

[10] Abdeljawad T, Mahariq I, Kavayanpoor M, Nazari MA, Bui DT. Identification of nonlinear normal modes for a highly flexible beam. Alex Eng J 2020;59:2419−27.

[11] Liu CX, Yan Y, Wang WQ. Primary and secondary resonance of a cantilever beam carrying an intermediate lumped mass with time delay feedback. Nonlinear Dynam 2019;97:1175−95.

[12] Amer YA, Bahanisy TA, Elmhlawy AM. On the existence of time delay for rotating beam with Proportional-Derivative Controller. Asian J Math 2021;17:99−122.

[13] Hamed YS, Albogamy KM, Sayed M. Nonlinear vibrations control of a contact-mode AFM model via a time-delayed positive position feedback. Alex Eng J 2021;60:963−77.

[14] Hamed YS, Albogamy KM, Sayed M. A proportional derivative (PD) controller for suppressing the vibrations of the a contact mode AFM model. IEEE Access 2020;8:214061−70.

[15] Amer YA, El-Sayed AT, Saleh AA, Abel-Wahab AM, Salaman HF. Positive position feedback controller for nonlinear beam subject to harmonically excitation. Asian Res J Math 2019;12:1−19.

[16] Amer YA, El-Sayed AT, Saleh AA, Abel-Wahab AM, Salaman HF. Vibrations control of the harmonically excited nonlinear system via positive position feedback controller. Al Azhar Bull Sci 2019;30:9−26.

[17] Mahmoodi NS, Ahmadian M. Active vibration control with modified positive position feedback. J Dyn Syst Meas Control 2009;131:1−8.

[18] Omidi E, Mahmoodi SN, JrWS Shepard. Multi positive feedback control method for active vibration suppression in flexible structures. Mechatronics 2016;33:23−33.

[19] Omidi E, Mahmoodi SN. Nonlinear vibration suppression of flexible structures using nonlinear modified positive position feedback approach. Nonlinear Dynam 2015;79:835−49.

[20] Hamed YS, El Shery A, Sayed M. Nonlinear modified positive position feedback control of cantilever beam system carrying an intermediate lumped mass. Alex Eng J 2020;59:3847−62.

[21] Mohanty S, Dwivedy SK. Traditional and non-traditional active-nonlinear vibration absorber with time delay combination feedback for hard excitation. Commun Nonlinear Sci Numer Simulat 2023;117:106916.

[22] Zhang W, Chen Y. Periodic response analysis of a Jeffcott-rotor system under modified saturation-based control. Commun Nonlinear Sci Numer Simulat 2023;116:106814.

[23] Saeed NA, Omara OM, Sayed M, Awrejcewicz J, Mohamed MS. Non-linear interactions of a Jeffcott-rotor system controlled by a radial PD-control algorithm and eight-pole magnetic bearings actuator. Appl Sci 2022;12:6688.

[24] Nayfeh AH, Mook DT. Nonlinear oscillations. New York: Wiley; 1995.

[25] Marinca V, Herisanu N. Nonlinear dynamical systems in engineering: some approximate approaches. USA: Springer Science & Business Media; 2012.